



Cite this: *Phys. Chem. Chem. Phys.*,
2017, 19, 14652

Metal nanoinks as chemically stable surface enhanced scattering (SERS) probes for the analysis of blue BIC ballpoint pens†

A. Alyami,^a D. Saviello,^a M. A. P. McAuliffe,^b A. Mirabile,^c L. Lewis^{ab} and D. Iacopino^{ib}*^a

Metal nanoinks constituted by Ag nanoparticles and Au nanorods were employed as probes for the Surface Enhanced Raman Scattering (SERS) analysis of a blue BIC ballpoint pen. The dye components of the pen ink were first separated by thin layer chromatography (TLC) and subsequently analysed by SERS at illumination wavelengths of 514 nm and 785 nm. Compared to normal Raman conditions, enhanced spectra were obtained for all separated spots, allowing easy identification of phthalocyanine Blue 38 and triarylene crystal violet in the ink mixture. A combination of effects such as molecular resonance, electromagnetic and chemical effects were the contributing factors to the generation of spectra enhanced compared to normal Raman conditions. Enhancement factors (EFs) between 5×10^3 and 3×10^6 were obtained, depending on the combination of SERS probes and laser illumination used. In contrast to previous conflicting reports, the metal nanoinks were chemically stable, allowing the collection of reproducible spectra for days after deposition on TLC plates. In addition and in advance to previously reported SERS probes, no need for additional aggregating agents or correction of electrostatic charge was necessary to induce the generation of enhanced SERS spectra.

Received 28th March 2017,
Accepted 30th April 2017

DOI: 10.1039/c7cp01983a

rsc.li/pccp

Introduction

The elucidation of ink composition in commercial ballpoint pens has been the object of forensic investigation for many years. However, recently this field of research has become increasingly relevant also for art conservation applications. Since their wide spread introduction in the market in 1945, ballpoint pens have been used as a versatile medium for artistic production, which are nowadays found in many museum collections all over the world. Unfortunately, inks suffer fast color fading when exposed to light and the proper conservation of ink-based artworks requires the development of novel active conservation and long-term preservation solutions. In this context, the identification of ink formulations is of paramount importance for the establishment of artwork's dating and originality as well as for the creation of ideal housing conditions towards deceleration of photo-degradation processes causing color fading.

Ballpoint pen inks are complex mixtures of several dyes and pigments constituting up to 50% of the total ink formulation contained in either a glycol-based solvent or benzyl alcohol.^{1,2} Additional components (vehicle) include fatty acids, softeners and polymeric resins, designed to improve the consistency, flow or drying characteristics of the ink.³ This complex composition makes the identification of dyes and pigments in inks challenging. Additional difficulties are constituted by trademark protection and periodical introduction in the market of novel products with slightly modified formulations.

The identification of inks used for artistic purposes requires the use of relatively low-cost, potentially deployable and non-destructive analytical techniques enabling *in situ* analysis and preservation of the analyzed object's integrity. For this reason spectroscopic techniques such as Fourier transform infrared (FTIR),^{4,5} X-ray fluorescence,⁶ and Raman spectroscopy^{7,8} are nowadays preferred to (or used in combination with) more conventional chromatography techniques. Among spectroscopic methods, Surface Enhanced Raman Scattering (SERS) has proven to be particularly amenable to the identification of ink mixtures, due to its ability to overcome the fluorescence interference observed in Raman and FTIR analyses. The SERS phenomenon is based on the enhancement of Raman signals experienced by analytes adsorbed on nanostructured metal surfaces. SERS arises from two contributions, an electromagnetic effect (EM) and a chemical

^a Tyndall National Institute, University College Cork, Dyke Parade, Cork, Ireland.
E-mail: Daniela.iacopino@tyndall.ie

^b Centre for Advanced Photonics & Process Analysis (CAPPA),
Cork Institute of Technology, Bishoptown, Cork, Ireland

^c Mirabile, 11 Rue de Bellefond, 75009 Paris 09, France

† Electronic supplementary information (ESI) available: Raman and SERS spectra of TLC separated spots at 514 nm and 785 nm illumination wavelengths. See DOI: 10.1039/c7cp01983a

effect (CE), leading to overall enhancements of up to 10^{12} compared to normal Raman (NR) signals.^{9–11} The largest enhancement factors were conventionally obtained with aggregated Ag spherical colloids whereas 1–2 orders of magnitude lower enhancements were reported for aggregated Au spherical particles.^{12,13} Accordingly, to date the majority of studies applied to the identification of ballpoint pens use Ag colloids as SERS probes. However, the efficacy of Ag colloids for SERS ink identification is still under debate with authors reporting poor reproducibility due to the fast oxidation of Ag colloids¹⁴ and others reporting good stability results.¹⁵ In addition, the following drawbacks were reported: measurements had to be performed within minutes of colloid deposition due to fast Ag oxidation, SERS signals were not reproducible due to inhomogeneous (coffee stain effect) evaporation of Ag colloidal droplets, and charged polymers had to be added to counter balance the negative surface charge of Ag colloids in order to promote electrostatic interaction with negatively charged dyes. In spite of this, alternative SERS probes based on more chemically stable materials have scarcely been proposed.¹⁶

Recently, theoretical work by Hao *et al.* calculated the greatest E-field enhancement at the end of isolated Au nanorods compared to other nanoparticle shapes, due to the high density of E-field concentrated at the nanorod tips.¹⁷ Other authors also referred to Au nanorods as the most promising candidates for the achievement of chemically stable and high intensity SERS signals.¹⁸ In parallel, Polavarapu *et al.* reported the synthesis of highly concentrated Au nanorod colloids which displayed stable and reproducible SERS spectra on paper substrates.¹⁹

In this paper we report on the use of chemically stable metal nanoinks for SERS analysis of a blue BIC ballpoint pen. Metal nanoinks were constituted by Ag nanospheres and Au nanorods and were used in combination with Thin Layer Chromatography (TLC) to identify the dye components in the pen. The novelty of this work relies in the clarification of chemical stability of metal nanoinks and the role played in the SERS effect observed by measuring the enhancement factors (EFs) arising from different effects at different excitation wavelengths. While normal Raman conditions required the use of two laser wavelengths to obtain the spectra of all separated spots on the TLC, SERS illumination at either 514 nm or 785 nm was successful in obtaining enhanced spectra for all separated spots. High intensity and good signal-to-noise SERS spectra were obtained, due to the matching of laser illumination with the plasmon resonance of the used nanoinks. In addition, the contribution of molecular resonance, electromagnetic and chemical effects was evaluated by further SERS analysis carried out under non-plasmonic resonance conditions. EFs between 5×10^3 and 3×10^6 were obtained for the separated spots, allowing identification of phthalocyanine Blue 38 and triarylene crystal violet (CV) in the pen ink mixture. In contrast with what is reported in the literature, both nanoinks gave stable SERS signals for days after deposition and did not necessitate the use of additional aggregating or charge-adjustment agents.

Results and discussion

Metal nanoinks used as SERS probes were synthesized by a modification of the synthesis reported by Polavaru *et al.*¹⁹ This method started with the synthesis of high volume nanoparticle solutions, which were subsequently concentrated up to 100 times in order to obtain highly viscous, ink-like solutions. Fig. 1 shows SEM images of Ag (1a) and Au (2a) nanoinks deposited on SiO₂ substrates. The Ag NIs were mostly spherical in shape and had an average size of 65 ± 3 nm; the Au NIs displayed an elongated (rod-like) shape with an average size of 13 ± 2 nm \times 41 ± 4 nm.

The separation of the dye components in the blue BIC pen ink was achieved by TLC (Fig. 2). By using an ethylacetate–ethanol–water (70:35:30 v/v) eluent blue spots and purple spots with retention factors (R_f) equal to = 0.44 and 0.67 formed by TLC as a result of ink mixture separation. For comparison, reference dyes solvent Blue 38 and CV were also deposited on the TLC and run alongside the pen spot. These dyes were specifically selected as triarylene dyes and phthalocyanine pigments were identified in the literature as components of the BIC ballpoint blue pen.^{14,20} Deposited Blue 38 displayed a R_f equal to = 0.44, whereas CV displayed R_f equal to = 0.67, equivalent to the R_f of the BIC blue and purple spots, respectively.

Prior to Raman analysis, absorbance spectroscopy was carried out in order to investigate the optical properties of the analytes and nanoinks. Fig. 3a shows the UV-vis spectrum of the BIC pen

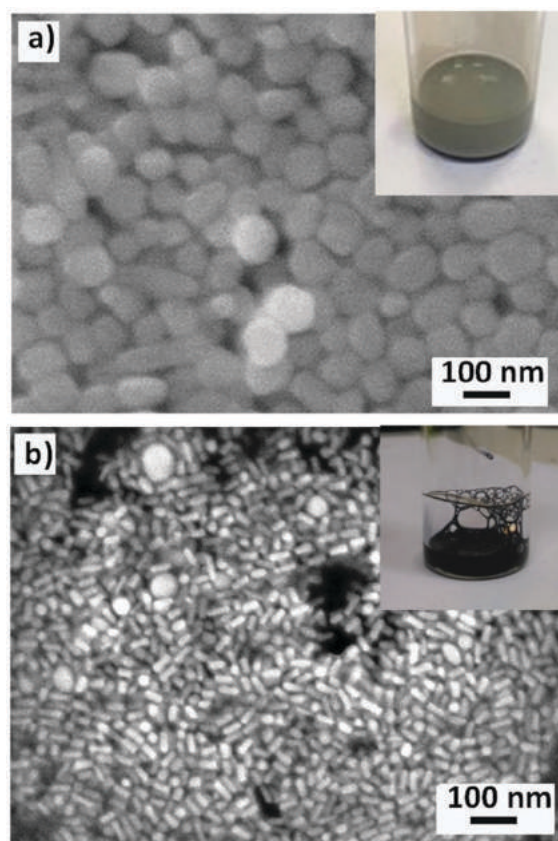


Fig. 1 SEM images of (a) Ag and (b) Au NIs deposited on SiO₂ substrates. Insets: Photographs of NI solutions. Metal colloids (nanoinks).

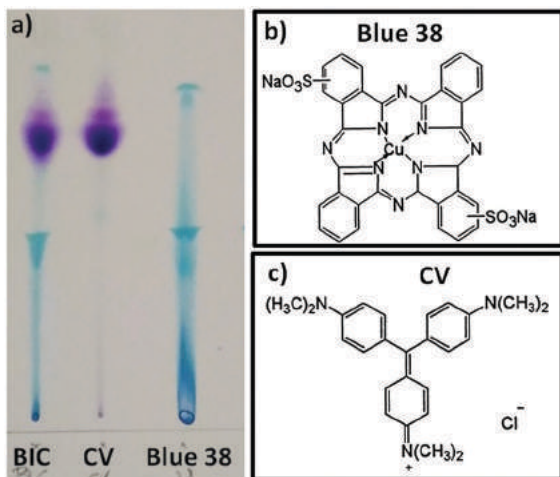


Fig. 2 (a) Photograph of TLC showing the BIC pen component and reference samples Blue 38 and CV; (b and c) molecular formulas of the reference samples Blue 38 and CV.

ink diluted in MeOH. The solution was intensely purple colored and showed a main peak centered at 588 nm with a shoulder at 548 nm, another peak was centered at 666 nm (buried under the CV peak in the pen solution spectrum) and 666 nm.²¹ CV showed the same peak and shoulder centered at 588 nm and 548 nm as shown by the BIC pen solution spectrum, arising from the coexistence of two isomeric forms in MeOH solution.²² Fig. 3b also shows the absorbance spectra of Ag NIs and Au NIs in water suspensions. The Ag NI solution was milky grey in color (see the inset of Fig. 1a) and was characterized by a relatively large plasmonic peak centered at 428 nm. The Au NI solution was deep blue in color (see the inset of Fig. 1b) and showed two peaks at 520 nm and 787 nm, characteristic of transversal and longitudinal plasmon resonances occurring in elongated nanoparticles.²³ As a result of this analysis two laser excitation wavelengths at 514 nm and 785 nm were selected for Raman analysis, as strongly enhanced SERS spectra were expected to be obtained, due to their plasmonic resonance with Ag and Au NIs, respectively (see dotted lines in Fig. 3b).

Fig. 4a shows Normal Raman (NR) spectra obtained by direct illumination of the TLC separated spots with an excitation wavelength of 514 nm (Fig. 4a). All spectra at 514 nm were recorded with a laser power of 2 mW and 10 s integration time. A featureless spectrum was obtained for the blue spot (light blue curve). A low intensity spectrum was also obtained for the reference Blue 38 with only two peaks appearing at 1539 cm^{-1} and 1337 cm^{-1} (dark blue curve). In contrast, the spectra of relatively good intensity were obtained for the purple spot and the reference CV (light purple and dark purple curves, respectively). Both spectra displayed the same diagnostic peaks at 1620 cm^{-1} , 1592 cm^{-1} , and 1540 cm^{-1} , associated with stretching of the benzene rings and 439 cm^{-1} and 420 cm^{-1} associated with bending of the CNC bonds.²⁴ The intensity of the observed spectra was ascribed to the occurrence of molecular resonance (MR) effects, due to the use of an illumination wavelength corresponding to a maximum in the absorption spectrum of CV

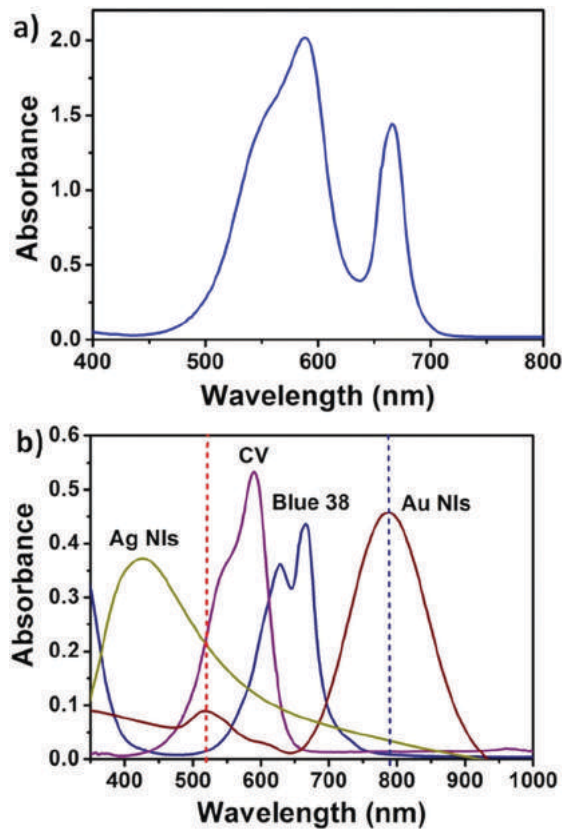


Fig. 3 (a) UV-vis spectrum of BIC pen solution in MeOH; (b) UV-vis spectra of Blue 38 and CV in MeOH and metal NIs in water. Dotted lines indicate the position of 514 nm (red) and 785 nm (blue) laser excitation wavelengths used for SERS analysis.

(Fig. 3b, red dotted line). These data allowed the preliminary identification of the purple spot as CV.

However, identification of the blue specimen was not possible under NR conditions. In contrast, Fig. 4b shows the SERS spectra of an equivalent TLC where Ag NIs were deposited in all spots and laser illumination of 514 nm was used as SERS excitation. Good SERS spectra with enhanced features were recorded for all spots. Specifically, the spectra of the blue spot and the Blue 38 spots previously not identifiable with NR, displayed highly enhanced features with peaks at 1605, 1526, 1453, 1405, 1338, and 605 cm^{-1} associated with internal vibrations of the phthalocyanine macrocycle.^{21,25} The intensity of the blue spot spectrum measured using the 1339 cm^{-1} peak as reference displayed a 2 orders of magnitude higher intensity compared to the intensity of the NR spectrum. This enhancement was attributed to an electromagnetic effect, due to the use of an illumination wavelength in plasmonic resonance with the Ag NIs (Fig. 3, red dotted line). The similarity between the spectra of the two blue specimens allowed unique identification of the blue spot as Blue 38. Similarly, the strong resemblance between the SERS spectra of purple specimens confirmed the identity of the purple spot as CV and highlighted the superior abilities of SERS for the identification of BIC pen components compared to NR spectroscopy. The spectrum of the purple spot was enhanced by 1 order of magnitude

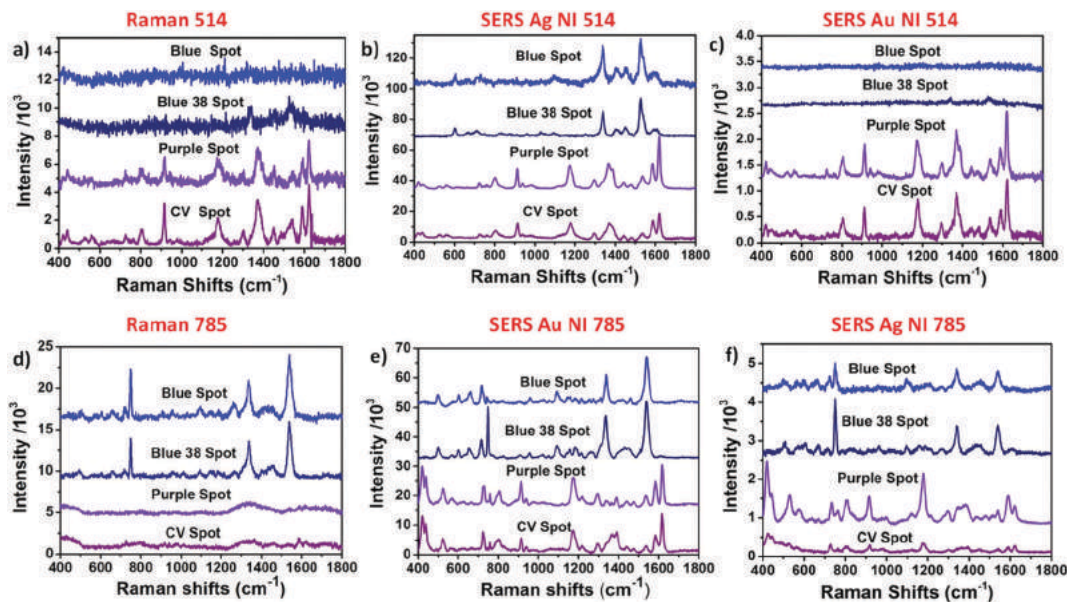


Fig. 4 NR and SERS spectra of TLC BIC pen components and reference samples Blue 38 and CV: (a) NR taken at an illumination wavelength of 514 nm; (b) SERS at 514 nm with Ag NIs; (c) SERS at 514 nm with Au NIs; (d) NR taken at an illumination wavelength of 785 nm; (e) SERS at 785 nm with Au NIs; (f) SERS at 785 nm with Ag NIs. Laser power was 2 mW and 35 mW for 514 nm and 785 nm lasers, respectively.

(measured at 1174 cm^{-1}) and displayed slightly red shifted peaks compared to NR conditions. The intensity of this spectrum was attributed to a combination of three effects: a molecular resonance (MR) effect; an electromagnetic effect (EM), due to the use of an illumination wavelength in plasmonic resonance with Ag NIs; and a chemical effect (CE), due to the formation of a chemical bond, and consequent charge transfer (CT), between CV and Ag *via* the central C atom whereby CV acted as an electron donor and Ag as the electron acceptor.²⁶ Proof of the occurrence of a charge transfer process was given by the observed red shift of frequencies displayed in the SERS spectrum compared to the NR spectrum (see Fig. S1b, ESI[†]). Specifically, the *N*-phenyl frequencies appearing at 1371 cm^{-1} and 1386 cm^{-1} in the NR spectrum were shifted to 1376 cm^{-1} and 1393 cm^{-1} , respectively in the SERS spectrum. Also the C=C ring frequency was shifted from 1619 cm^{-1} to 1627 cm^{-1} . Further proof of the occurrence of a CT process was given by the predominant enhancement of the non-totally symmetric (e) modes compared to the totally symmetric (a_1) modes.²⁴ In order to acquire more detailed information on the three effects the SERS spectra of an equivalent TLC plate were also recorded under non-plasmonic resonance conditions by substituting Ag NIs with Au NIs, which was characterized by a plasmonic resonance of 790 nm (see Fig. 3b). The SERS spectra of all TLC colored spots (Fig. 3c) at 514 nm with Au NIs were equivalent to the Raman spectra recorded at 514 nm (Fig. 3a), indicating that no SERS effect occurred due to the absence of plasmonic resonance conditions. Under these conditions, the intensities displayed by the purple and CV spectra could be entirely attributed to a MR contribution. A parallel comparison was carried out at an illumination wavelength of 785 nm. All spectra at 785 nm were recorded with a laser power of 35 mW and 10 s integration time. Fig. 4d shows the NR spectra of BIC pen

separated spots directly measured on a TLC plate. The spectra obtained were somehow complementary to those obtained for NR illumination at 514 nm. The blue spot and Blue 38 specimens displayed good spectra (light and dark blue curves, respectively) characterized by the same diagnostic peaks at 1539 cm^{-1} , 1340 cm^{-1} and 720 cm^{-1} . In contrast, the spectrum of the purple spot displayed no features and the spectrum of the reference CV displayed only small peaks around 1600 cm^{-1} . Similarly to what was observed under NR conditions at a 514 nm illumination wavelength, NR at 785 nm was not able to identify all separated spots in the BIC pen and only preliminary identification of the blue spot as Blue 38 was possible. As comparison, Fig. 4e shows the SERS spectra of the same TLC where Au NIs were deposited in all separated spots and 785 nm was used as SERS excitation. The spectra of the blue specimens, already visible under NR conditions, appeared to be enhanced due to the use of an illumination wavelength in plasmonic resonance with Au NIs (EM effect) and showed additional peaks compared to the spectra recorded under NR conditions. The additional peaks belonged to asymmetric modes of symmetry a_{2g} , which were reported to occur only in concomitance to the occurrence of a charge transfer process (see Fig. S1c, ESI[†]).²⁷ Therefore, the enhancement observed was attributed to a combination of EM and CE effects. This enhancement allowed the unique identification of the blue specimen as Blue 38. The purple spot and CV showed highly enhanced spectra compared to NR conditions with peaks in the same positions as discussed in Fig. 3a, thus confirming the identity of the purple spot as CV. Thus once again at 785 nm illumination SERS was superior to NR spectroscopy in enabling fast and sensitive identification of BIC pen ink components. The enhancement observed for the purple spot was entirely due to an EM effect. It should be pointed out here that CV would also be able

Table 1 Relative intensity of reference peaks and contribution effects for blue and purple specimens measured under all experimental conditions

	Blue specimen		Purple specimen	
	Intensity (1339 cm ⁻¹)	Contributions	Intensity (1174 cm ⁻¹)	Contributions
Raman 514 nm	105	—	1189	MR
SERS Ag 514 nm	12 895	EM	15 510	MR, EM, CT
SERS Au 514 nm	25	—	743	MR
Raman 514 nm	1974	—	231	—
SERS Au 785 nm	9252	EM, CT	4525	EM
SERS Ag 785 nm	498	—	1304	CT

to form a CT complex with Au *via* the N groups.²⁶ However, no evidence of the CT effect was observed in the spectra (*i.e.* no changes compared to the corresponding NR spectrum observed, see the ESI[†]), likely prevented by the electrostatic repulsion originating by the double positive charge of CV and Au nanorods. For completion, the SERS spectra of all TLC colored spots (Fig. 4e) were recorded under non-plasmonic resonance conditions (*i.e.* at 785 nm with Ag NIs). The spectrum of the blue spot showed 1 order of magnitude lower intensity than the equivalent SERS spectrum recorded at 785 nm with Au NIs, due to the absence of EM resonance. The spectrum of the purple spot showed peaks of slightly lower intensity than those recorded under resonance conditions (absence of EM contribution) but of higher intensity than those recorded under NR conditions at 785 nm. This enhancement was ascribed only to a charge transfer process (CE effect) occurring between CV and Ag nanoparticles discussed earlier as laser excitation (785 nm) was far removed from the plasmonic absorption of Ag NIs and the absorption maximum of CV (see Fig. 3b) to see contributions from MR and EM effects.

The relative intensities of the reference peaks and the contributions of the various effects measured under all experimental conditions for the blue and purple specimens are summarized in Table 1.

A further quantification of the SERS process was carried out by calculating the enhancement factor (EF), defined as the ratios of the intensities of the scattered radiation for SERS and normal Raman scattering per molecule

$$EF = (I_{\text{SERS}}/N_{\text{SERS}})/(I_{\text{NR}}/N_{\text{NR}})$$

where I_{SERS} and I_{NR} are the integrated intensities of the SERS and normal Raman scattering spectra for Blue 38 and CV (Table 1); N_{SERS} and N_{NR} are the number of molecules found in the laser excitation area adsorbed on Ag/Au NI and on TLC, respectively. EFs were calculated following the method adopted by Kim *et al.*²⁸ and by considering 0.5 nm² and 0.1 nm² the area occupied by one Blue 38 and one CV molecule, respectively.^{29,30} The calculated EFs for all experimental conditions are reported in Table 2.

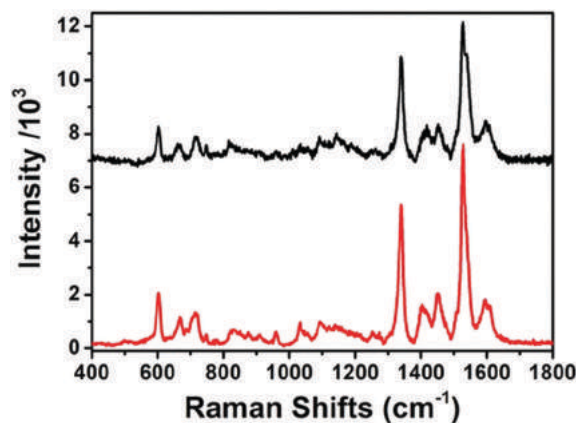
In the case of the purple spot (CV) Table 1 suggests that the contribution of the MR to the overall enhancement can be calculated under non-resonance conditions (SERS Au NIs, 514 nm) and it is equal to 2.2×10^4 . This value should be added to the EF calculated under resonance conditions (7.5×10^4), which comprises the contributions of EM and CT. Therefore, the total EF under resonance conditions, EF_{R} , would

Table 2 EFs of blue and purple specimens calculated for all experimental conditions

	Blue spot EFs	Purple spot EFs
SERS Ag NIs, 514 nm	2.6×10^6	7.5×10^4
SERS Au NIs, 785 nm	1.0×10^5	1.1×10^5
SERS Au NIs, 514 nm	—	2.2×10^4
SERS Ag NIs, 785 nm	5.5×10^3	3.2×10^4

be 9.7×10^4 . Considering that the CT contribution obtained under non-resonance conditions (SERS Ag NIs, 785 nm) was equal to 3.2×10^4 , it was possible to calculate the EM contribution to be equal to 4.3×10^4 ($EM = EF_{\text{R}} - MR - CT = 9.7 \times 10^4 - 2.2 \times 10^4 - 3.2 \times 10^4$).

In order to clarify some of the contrasting reports from the literature, SERS spectra with Ag NIs were acquired following multiple illumination steps and days after nanoink deposition. Fig. 5 shows the SERS spectrum of a blue spot recorded at 514 nm (back line) and an equivalent spectrum recorded after three days (red line) displaying reproducible and intensity-comparable features. No degradation or oxidation of SERS probes was observed, provided that the TLC was stored in the dark to prevent dye color fading. Equally, Au NIs were chemically stable and TLC spots could be illuminated after four weeks of nanoink deposition. Furthermore, for both nanoinks no use of aggregating agents was necessary and no adjustment of electrostatic charge had to be made to promote a chemical link with charged analytes (*i.e.* between negatively charged Ag NIs and Blue 38 and positively charged Au NIs and CV).

**Fig. 5** SERS spectra of a TLC blue spot taken after 10 min Ag NI deposition (black line) and after three days of Ag NI deposition (red line).

Experimental

Materials

Tetrachloroauric acid, silver nitrate, sodium citrate, sodium borohydride, ascorbic acid, cetyltrimethyl-ammoniumbromide (CTAB), and MeOH were purchased from Sigma-Aldrich. All glassware was cleaned with aqua regia prior to nanoink synthesis. Milli-Q water (resistivity $> 18 \text{ M}\Omega \text{ cm}^{-1}$) was used throughout the experiments. Reference dyes Blue 38 and CV were also purchased from Sigma and used without further purification.

Synthesis of metal nanoinks (NIs)

Silver NIs were synthesized by a modification of the Lee and Meisel method reported by Polavarapu *et al.*¹⁹ Au nanorod NIs were synthesized by a modification of the seed mediated growth reported by Polavarapu *et al.*¹⁹ Specifically, a seed solution was prepared by adding 0.3 mL of an ice-cold aqueous sodium borohydride (NaBH_4 , 0.01 M) solution to an aqueous solution of 4.7 mL hexadecyltrimethylammonium bromide (CTAB, 0.1 M) and 25 μL of gold(III) chloride trihydrate (HAuCl_4 , 0.05 M) at 30 °C. An aliquot of 0.36 mL of the seed solution was added to a growth solution prepared by mixing 150 mL of CTAB (0.05 M), 1.5 mL of HAuCl_4 (0.05 M), 0.225 mL of silver nitrate (AgNO_3 , 0.01 M) and 5.0 mL of ascorbic acid (0.1 M) at 30 °C. The solution color changed from colorless to brownish-bluish after the addition of the seed solution to the brown solution. The obtained aqueous solution of gold nanorods was centrifuged twice and redispersed in water (1 mL) to get the nanorod ink.

Scanning electron microscopy (SEM) images of nanoinks deposited on SiO_2 substrates were acquired using a field emission SEM (JSM-6700F, JEOL UK Ltd) operating at beam voltages of 2 kV.

Thin layer chromatography was performed with silica plates $10 \times 20 \text{ cm}$ (Sigma-Aldrich). The BIC ballpoint pen and reference samples were deposited as concentrated MeOH solutions. TLC was performed in ethylacetate–ethanol–water (70 : 35 : 30 v/v) for 60 min.

Optical characterization

UV-vis spectra were acquired using an Agilent/HP 8453 UV-vis Spectrophotometer (200 nm $< \lambda < 1100 \text{ nm}$). Raman spectra at 514 nm were obtained from a Renishaw inVia Raman system. A helium–neon laser was employed as an excitation source. The laser beam was focused onto the sample through a Leica 20X objective with 0.4 N.A. Measured power at the sampling level was controlled at about 3 mW. Acquisition time was usually 10 s. Raman spectra at 785 nm were obtained from a Pelkin Elmer Raman station. The laser beam was focused onto the sample through a 50 \times objective (M Plan Achromat) with 0.75 N.A. The laser power was around 35 mW and typical acquisition time was 10 s. To obtain SERS spectra, 5 μL of metal nanoinks were deposited on the TLC plate and left to evaporate for 10 minutes prior to the analysis.

Conclusions

In conclusion we have applied SERS to the analysis of a blue ballpoint BIC pen. When used in combination with TLC, a strong enhancement of Raman signals was obtained for two

excitation wavelengths at 514 nm and 785 nm which enabled the easy identification of Blue 38 and CV in the ink mixture. Enhancement factors of up to 1×10^6 were obtained with the two lasers, and were due to a combination of effects, depending on the experimental conditions used. The strongest enhancements were obtained under plasmonic resonance conditions and were therefore associated with the use of stable metal nanoinks as SERS probes. The used Ag NIs and Au NIs were chemically stable, did not necessitate the addition of aggregating or binding agents to display SERS effects, and could be used for days after deposition displaying reproducible features. The developed probes offer an alternative to existing analytical tools for the reliable, fast and low cost analysis of ballpoint pens and concomitantly open the way for the analysis of trace amounts particularly relevant for forensic and art applications.

Acknowledgements

This work was funded by the European Union H2020 project Nanorestart (646063) and the Irish Research Council (IRC) project GOIPD/2015/716.

Notes and references

- 1 J. A. Siegel and P. J. Saukko, *Encyclopedia of Forensic Sciences*, Academic Press, Waltham, 2013, p. 375.
- 2 R. A. Merrill and E. G. Bartick, *J. Forensic Sci.*, 1992, **37**, 528.
- 3 S. Bell, *Encyclopedia of Forensic Sciences*, Infobase Publishing, New York, 2008.
- 4 J. Zięba-Palus and M. Kunichi, *Forensic Sci. Int.*, 2006, **158**, 164.
- 5 W. Dirwono, J. S. Park, M. R. Augustin-Camacho, J. Kim, H. M. Park, Y. Lee and K. B. Lee, *Forensic Sci. Int.*, 2010, **199**, 6.
- 6 S. Dhara, N. L. Misra, S. D. Maind, S. A. Kumar, N. Chattopadhyay and S. K. Aggarwal, *Spectrochim. Acta, Part B*, 2010, **65**, 167.
- 7 A. Braz, M. López-López and C. García-Ruiz, *Forensic Sci. Int.*, 2013, **232**, 206.
- 8 I. Geiman, M. Leona and J. R. Lombardi, *Forensic Sci.*, 2009, **54**, 947.
- 9 D. L. Jeanmaire and R. P. Van Duyne, *J. Electroanal. Chem.*, 1977, **84**, 1.
- 10 K. Kneipp, H. Kneipp, I. Itzkan, R. R. Dasari and M. S. Feld, *Chem. Rev.*, 1999, **99**, 2957.
- 11 C. J. Orendoff, L. Gearheart, N. R. Jana and C. J. Murphy, *Phys. Chem. Chem. Phys.*, 2006, **8**, 165.
- 12 X. H. Xu, E. J. Bjerneld, M. Kall and L. Borjesson, *Phys. Rev. Lett.*, 1999, **83**, 4357.
- 13 J. Jiang, K. Bosnick, M. Maillard and L. Brus, *J. Phys. Chem. B*, 2003, **107**, 9964.
- 14 R. M. Seifar, J. M. Verheul, F. Ariese, U. A. Th. Brinkman and C. Gooijer, *Analyst*, 2001, **126**, 1418.
- 15 P. C. White, *Sci. Justice*, 2003, **43**, 149.
- 16 Z. Luo, J. C. Smith, T. M. Goff, J. H. Adair and A. W. Castleman Jr., *Chem. Phys.*, 2013, **423**, 73.
- 17 E. Hao and C. G. J. Schatz, *Chem. Phys.*, 2004, **120**, 357.

- 18 C. J. Murphy, T. K. Sau, A. M. Gole, C. J. Orendoff, J. Gao, L. Gou, S. E. Hunyadi and T. Li, *J. Phys. Chem. B*, 2005, **109**, 13857.
- 19 L. Polavarapu, A. La Porta, S. N. Novikov, M. Coronado-Purchau and L. M. Liz-Marzán, *Small*, 2014, **15**, 3065.
- 20 M. Gallidabino, C. Weyermann and R. Marquis, *Forensic Sci. Int.*, 2011, **204**, 169.
- 21 B. Brożek-Pluska, I. Szymczyk and H. Abramcz, *J. Mol. Struct.*, 2005, **744–747**, 481.
- 22 G. N. Lewis, T. T. Magel and D. Lipkin, *J. Am. Chem. Soc.*, 1942, **64**, 1774.
- 23 S. Eustis and M. A. El-Sayed, *Chem. Soc. Rev.*, 2006, **35**, 209.
- 24 M. V. Canamares, C. Chenal, R. L. Birke and J. R. Lombardi, *J. Phys. Chem. C*, 2008, **112**, 20295.
- 25 D. Li, Z. Peng, L. Deng, Y. Shen and Y. Zhou, *Vib. Spectrosc.*, 2005, **39**, 191.
- 26 P. Selvakannan, R. Ramanathan, B. J. Plowman, Y. M. Sabri, H. K. Daima, A. P. O'Mullane and V. B. S. Bhagava, *Phys. Chem. Chem. Phys.*, 2013, **15**, 12920.
- 27 P. Corio, J. C. Rubin and R. Avoca, *Langmuir*, 1998, **14**, 4162.
- 28 K. Kim, H. B. Lee, J. Y. Choi, K. L. Kim and K. S. Shin, *J. Phys. Chem. C*, 2011, **115**, 13223.
- 29 M. V. Rivas, L. P. Méndez De Leo, M. Hamer, R. Carballo and F. J. Williams, *Langmuir*, 2011, **27**, 10714.
- 30 https://pubchem.ncbi.nlm.nih.gov/compound/Crystal_violet#section=Chemical-and-Physical-Properties.